The Reactivity of Defects at the Sidewalls of Single-Walled Carbon Nanotubes: The Stone–Wales Defect

Holger F. Bettinger*

Lehrstuhl für Organische Chemie II, Ruhr-Universität Bochum, 44780 Bochum, Germany

Received: December 31, 2004; In Final Form: March 10, 2005

The reactivity of 5/7/7/5 (Stone–Wales, SW) defects is compared to that of the pristine sidewalls of (5,5) and (10,0) carbon nanotubes (CNTs) using density functional theory (PBE). Infinite tube models (periodic boundary conditions) are used to investigate the reaction energy for CH_2 addition to the ten [5,6], [5,7], [6,7], and [7,7] C–C junctions resulting from SW rotations of the two unique bonds in (5,5) and (10,0) CNTs. In all cases, at least one of the junctions associated with the SW defects is more highly reactive than the pristine tubes. The orientation of these junctions with respect to the tube axis mainly determines the exothermicity. The [7,7] junctions are not the most reactive sites in SW defects of (5,5) and (10,0) CNTs.

Introduction

Defects, formed inevitably during the growth of carbon nanotubes (CNTs) or introduced during workup (e.g., oxidative cleaning, ultrasonication), have long been recognized to influence the physical properties of CNTs.[1–4] It is also known that defects have a substantial influence on the observed chemical behavior of CNTs,[5,6] and attempts have been made to visualize defects by binding nanoscale clusters.[7,8] Defects are also important in the oxidative functionalization and shortening of CNTs,[9] and Li et al. have given a detailed analysis of the dependence of defect density on the oxidation conditions.[8] According to these workers, mildly oxidizing acids attack the single-walled nanotube (SWNT) caps and defect sites. More strongly oxidizing conditions, possibly in combination with ultrasonication, can result in newly formed defect sites, which in turn can function as nuclei for further chemical etching. Consequently, such procedures generally go along with substantial shortening of the SWNT. While the defects involved in these chemical processes cannot be characterized in detail, four groups of defects are generally considered: topological (ring sizes other than hexagons), rehybridization (sp^2 and sp^3 hybridization of carbon), incomplete bonding (vacancies), and doping defects.[3]

A very important topological defect in carbon nanotube science is a pentagon–heptagon pair, also called a Stone–Wales (SW) defect, which is accessible from the pristine structure by a 90° rotation of a C_2 unit, the SW transformation.[10]
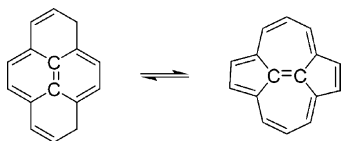
The interaction of atoms and molecules with defect sites has been considered in some previous theoretical investigations, first in the context of SW defects in [60]fullerene by Slanina et al.,[11] but later also for CNTs.[12–21] Of particular interest here are the studies of oxygen,[17–19,21] ozone,[14,19] and acetone[6] adsorption to an SW defect in (10,0) and (5,5) CNTs. However, a significant impact of defects is also anticipated for chemical functionalization of CNTs with carbenes,[22–25] nitrenes,[26,27] and oxygen atoms. It has been shown previously for armchair tubules that the addition of such divalent species shows pronounced dependence on the orientation of the [6,6] bond with respect to the tube axis.[28–30] The addition to the circumferential bond A (Figure 1) is more exothermic by 29 and 12 kcal mol^{-1} than to the axial bond B for (5,5) and (10,10) tubes, respectively.[28] Consequently, the orientations of bonds **1**–**10** associated with the defects relative to the tube axis could have an effect on the addition energy, and hence the reactivity, rivaling the inherent reactivity of the [*n*,*m*] junction. We present here a density functional theory (DFT) study of the reactivity towards methylene, CH_2, of the various SW defect sites possible in (5,5) and (10,0) SWNTs. As there are two distinct bonds in armchair and zigzag SWNTs, SW transformations can give rise to two distinct 5/7/7/5 defects, which differ by their orientation with respect to the tube axes. In defect A, the circumferential bond A is the one which underwent rotation, while the rotation of the axial bond B results in defect B.

Defects (5,5)-A and (10,0)-B have local C_{2v} symmetry, and thus for each of these defected tubes, six new symmetrically unique ring junctions result: two [5,6] (**1, 2**), one [5,7] (**3**), two [6,7] (**5, 6**), and one [7,7] (**4**) junction. Defects (5,5)-B and (10,0)-A only have local C_2 symmetry, and thus, four more symmetrically unique bonds **7**–**10** exist in these defects. To explore the reactivity of these 5/7/7/5 defects, addition to all of these newly generated sites (labeled as in Chart 1) has to be taken into account.

Theoretical Methods

The (5,5) and (10,0) SWNTs were modeled by imposing periodic boundary conditions (PBCs) as implemented in the

* E-Mail: Holger.Bettinger@rub.de. Fax: +49 234 321 4353.

Letters

J. Phys. Chem. B, Vol. 109, No. 15, 2005 **6923**
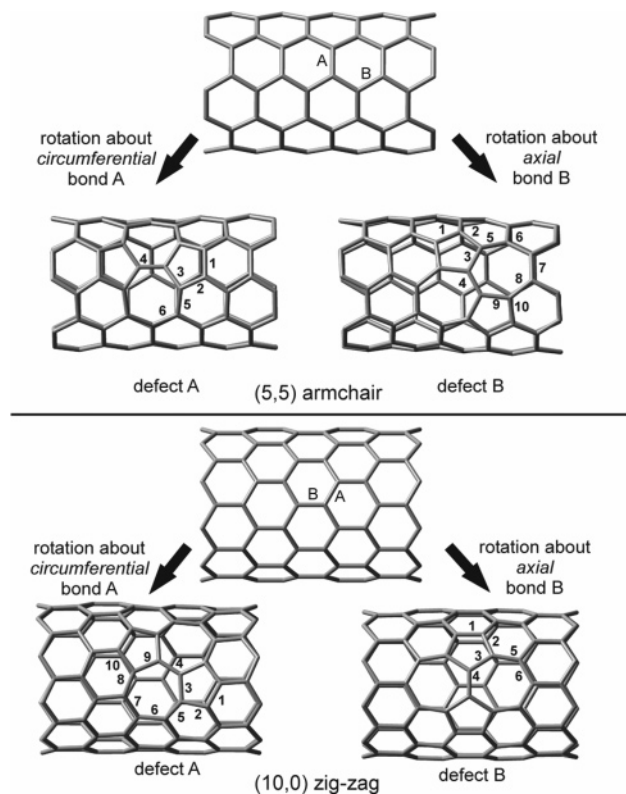
Figure 1. Armchair (top) and zigzag (bottom) carbon nanotubes and the defects (A and B) resulting from rotation about *circumferential* bonds A and *axial* bonds B, respectively.

CHART 1: Labeling of the [5,6] (1, 2), [5,7] (3), [6,7] (5, 6), and [7,7] (4) Junctions Newly Formed at the Sidewalls of Carbon Nanotubes upon Stone–Wales Transformation
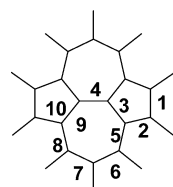
Gaussian 03 program[31] to simulate tubes of infinite lengths. The unit cell chosen consists of 100 and 120 carbon atoms for (5,5) and (10,0) tubes, respectively, while the integration of **k** space was achieved by using the default number of **k** points, 27 and 26, respectively. The geometries were optimized using the PBE[32,33] functional and the 3-21G basis set, while final energies were computed with the 6-31G* basis set (i.e., PBE/6-31G*//PBE/3-21G). The PBE/3-21G method gave geometries for carbene addition to pristine sidewalls in qualitative agreement with B3LYP/6-31G* data, in particular, with respect to the formation of three-membered rings (cyclopropanation) or C–C insertion.[28,29] Spin-unrestricted computations were performed for the triplet state of methylene, which was used to evaluate the addition energies for CNT + $CH_2(^3B_1) \rightarrow$ CNT–CH_2, while the CNT and CNT–CH_2 adducts were computed in their singlet states.

Results and Discussion

We first consider the SW defect "free" from the surrounding graphitic lattice (i.e., the $C_{16}H_{10}$ hydrocarbon azupyrene) as a reference system. The C–C distances in $C_{16}H_{10}$ range between 1.38 Å for the central bond **4** and 1.48 Å for bond **3**, while perimeter bonds **1**, **2**, **5**, and **6** have lengths in the 1.39–1.44 Å

TABLE 1: Energies (in kcal mol^{-1}) Computed at the PBE/6-31G*//PBE/3-21G Level of Theory for the Addition Reaction C_{20n} + $CH_2(^3B_1) \rightarrow C_{20n}CH_2$ to Bonds 1–10 Associated with 5/7/7/5 Defects A and B Resulting from Rotation of Circumferential (A) and Axial (B) Bonds, Respectively (see Chart 1 and Figure 1), in an Infinite (5,5) Armchair (C_{100}, $n = 5$), an Infinite (10,0) Zigzag Tube (C_{120}, $n = 6$), and in Azupyrene ($C_{16}H_{20}$), the Defect "Free" from the Surrounding Graphitic Lattice

addition site	azupyrene, $C_{16}H_{10}$	(5,5) defect A	(5,5) defect B	(10,0) defect A	(10,0) defect B
1	−82.1	−97.8	−69.6	−78.3	−65.1
2	−63.1	−84.0	−82.4	−85.5	−77.8
3	−73.4	−61.2	−113.2	−86.3	−99.7
4	−80.6	−62.5	−88.5	−66.3	−99.0
5	−74.7	−101.1	−74.5	−70.9	−78.9
6	−76.1	−67.6	−65.4	−69.6	−93.5
7			−109.6	−77.7	
8			−91.8	−98.4	
9			−82.2	−59.0	
10			−85.6	−79.1	
perfect tube		−97.5^a	−68.7^a	−67.2^a	−76.9^a

^{a} Addition to the corresponding bond in the pristine CNT (see Figure 1).

range. The methylene addition reactions are exothermic and generally result in cyclopropane derivatives, while an insertion into the C–C bond ($r = 2.320$ Å) is obtained for the [5,7] junction **3**. The [7,7] junction **4** is special among the 6 unique bonds of the azupyrene molecule, and most previous computational investigations on the defect reactivity in CNTs focused on this bond. Addition to it results in a 14-electron Hückel-aromatic ($4n + 2$, $n = 3$) perimeter (the bond length alternation is only 0.027 Å), but **4**–CH_2 is only the second most favorable adduct after **1**–CH_2 (Table 1). Site **2** is least reactive, and **3**, **5**, and **6** show similar and intermediate reactivity.

Embedding the SW defect into the graphitic lattice of the (5,5) and (10,0) CNTs has several consequences: (i) the central C–C bond **4** remains the shortest bond by far (1.34–1.38 Å), while bond **3** is almost exclusively the longest (the exception being (5,5)-A-**6**); (ii) methylene inserts into at least one bond in all of the four defects considered; (iii) the reaction energies change and differ significantly for the various bonds of defects A and B. A more detailed look reveals that the insertion versus addition, and along with this the exothermicities, depend on the orientation of the bonds within the defects with respect to the tube axis.

In (5,5)-A, the most exothermic reactions are obtained for site **5**, followed by **1**. The reaction with methylene results in insertion into these C–C bonds (typical CC distances are greater than 2.2 Å), while the **2**, **4**, **5**, and **6** C–C bonds react under cyclopropane formation (i.e., the carbene adds to these bonds without breaking them) resulting in CC distances shorter than 1.58 Å.[28,29] The [7,7] junction **4**, which is among the most reactive sites in the reference system azupyrene, shows low reactivity and undergoes cyclopropane formation with a rather short bridgehead distance of 1.39 Å in (5,5)-A-**4**–CH_2. For comparison, reaction with the (5,5)-B-**4** site is more highly exothermic, and a somewhat longer bridgehead C–C bond (1.55 Å) results in (5,5)-B-**4**–CH_2. This variation in lengths and addition energies should reflect the different amounts of strain exerted on bonds **4** due to their different orientation with respect to the tube axes in (5,5)-A and (5,5)-B. An additional factor is the local deformation at (5,5)-A-**4**: the two carbon atoms have moved away from the tube surface toward the tube center. The pyramidalization angle[34] of these carbon atoms is thus reduced (2.8° vs 6.0° in the pristine (5,5) tube), causing a decreased

reactivity toward exohedral attack. The least reactive site of (5,5)-A is **3**, but this is, together with **7**, most reactive in defect (5,5)-B. As in azupyrene, C−C bond insertion is observed at site **3** in defects (5,5)-A and (5,5)-B. Similarly, sites **5** and **1** (most reactive in (5,5)-A) have low reactivity in (5,5)-B. Hence, the nature of the ring junction (i.e., [5,7] vs [6,7]) is not decisive for exothermicities and adduct geometries. Rather, the orientation of the bonds relative to the tube axis seems to determine the reactivity: both **5** and **1** are oriented most closely to being orthogonal to the tube axis in (5,5)-A. They are thus most highly strained and have the highest reactivity. Similarly, bonds **7** and **3** in (5,5)-B have circumferential orientation and are most highly strained and most reactive.

The importance of bond orientation is also observed for the zigzag tubes. Bonds **8** and **3** have circumferential orientation in (10,0)-A, and the insertion into them is the most strongly exothermic reaction. The [6,7]-junction **8** is slightly more reactive than the [5,7] bond **3**. While site (10,0)-A-**9** is less reactive than bonds A and B in the pristine (10,0) tube, all bonds associated with defect (10,0)-A are more reactive. In the (10,0)-B defect, the [7,7]-junction **4** has circumferential orientation, resulting in a highly exothermic carbene addition reaction (-99.0 kcal mol^{-1}). Bond **4** in (10,0)-B is very short (1.378 Å) and can thus be considered as a double bond flanked by single bonds **3** (1.518 Å). Consequently, reaction with CH$_2$ results in a cyclopropane derivative (10,0)-**4**−CH$_2$ ($r = 1.587$ Å) and a C−C insertion product ($r = 2.303$ Å) for **3**. The latter reaction is even slightly more exothermic (-99.7 kcal mol^{-1}) than addition to (10,0)-**4**. Bond (10,0)-B-**6**, a [6,7]-junction, has an orientation similar to a pristine bond A but shows a significantly higher exothermicity (-93.5 kcal mol^{-1}) for C−C bond insertion (r(CC) $= 2.289$ Å).

Conclusions

In conclusion, the expectation that 5/7/7/5 defects are more highly reactive than pristine tube walls is confirmed for the reaction with methylene. However, it is also important to realize that significant differences among the addition sites newly generated by the Stone-Wales transformation exist: while some of the bonds show higher reactivity than those in the pristine tubes, others are less reactive. The relative orientations of the 5/7/7/5 dislocation dipoles and, as a consequence, of the newly generated addition sites with respect to the tube axis is more important than the nature of the ring junction ([5,6], [5,7], [6,7], and [7,7]). Nonetheless, favorably oriented [6,7] junctions are often ((5,5)-A, (5,5)-B, and (10,0)-A) most reactive. The [7,7] junctions have been the focus of previous investigations, but for all cases investigated, other bonds are found to be more reactive.

References and Notes

(1) Ebbesen, T. W.; Takada, T. *Carbon* **1995**, *33*, 973.
(2) Louie, S. G. *Top. Appl. Phys.* **2001**, *80*, 113.
(3) Charlier, J.-C. *Acc. Chem. Res.* **2002**, *35*, 1063.

(4) Watts, P. C. P.; Hsu, W.-K.; Kroto, H. W.; Walton, D. R. M. *Nano Lett.* **2003**, *3*, 549.
(5) Bom, D.; Andrews, R.; Jacques, D.; Anthony, J.; Chen, B.; Meier, M. S.; Selegue, J. P. *Nano Lett.* **2002**, *2*, 615.
(6) Chakrapani, N.; Zhang, Y. M.; Nayak, S. K.; Moore, J. A.; Carroll, D. L.; Choi, Y. Y.; Ajayan, P. M. *J. Phys. Chem. B* **2003**, *107*, 9308.
(7) Fan, Y.; Burghard, M.; Kern, K. *Adv. Mater.* **2002**, *14*, 130.
(8) Li, X.; Niu, J.; Zhang, J.; Li, H.; Liu, Z. *J. Phys. Chem. B* **2003**, *107*, 2453.
(9) Liu, J.; Rinzler, A. G.; Dai, H.; Hafner, J. H.; Bradley, R. K.; Boul, P. J.; Lu, A.; Iverson, T.; Shelimov, K.; Huffman, C. B.; Rodriguez-Macias, F.; Shon, Y.-S.; Lee, T. R.; Colbert, D. T.; Smalley, R. E. *Science* **1998**, *280*, 1253.
(10) Stone, A. J.; Wales, D. J. *Chem. Phys. Lett.* **1986**, *128*, 501.
(11) Slanina, Z.; Zhao, X.; Uhlik, F.; Ozawa, M.; Osawa, E. *J. Organomet. Chem.* **2000**, *599*, 57.
(12) Meng, F. Y.; Zhou, L. G.; Shi, S.-Q.; Yang, R. *Carbon* **2003**, *41*, 2023.
(13) Nevidomskyy, A. H.; Csányi, G.; Payne, M. C. *Phys. Rev. Lett.* **2003**, *91*, 105502.
(14) Picozzi, S.; Santucci, S.; Lozzi, L.; Valentini, L.; Delley, B. *J. Chem. Phys.* **2004**, *120*, 7147.
(15) Fagan, S. B.; da Silva, A. J. R.; Mota, R.; Baierle, R. J.; Fazzio, A. *Phys. Rev. B* **2003**, *67*, 033405.
(16) Zhou, L. G.; Shi, S.-Q. *Carbon* **2003**, *41*, 613.
(17) Grujicic, M.; Cao, G.; Singh, R. *Appl. Surf. Sci.* **2003**, *211*, 166.
(18) Grujicic, M.; Cao, G.; Rao, A. M.; Tritt, T. M.; Nayak, S. *Appl. Surf. Sci.* **2003**, *214*, 289.
(19) Lu, X.; Chen, Z.; Schleyer, P. v. R. *J. Am. Chem. Soc.* **2005**, *127*, 20.
(20) Valentini, L.; Mercuri, F.; Armentano, I.; Cantalini, C.; Picozzi, S.; Lozzi, L.; Santucci, S.; Sgamellotti, A.; Kenny, J. M. *Chem. Phys. Lett.* **2004**, *387*, 356.
(21) Giannozzi, P.; Car, R.; Scoles, G. *J. Chem. Phys.* **2003**, *118*, 1003.
(22) Chen, J.; Hamon, M. A.; Hu, H.; Chen, Y.; Rao, A. M.; Eklund, P. C.; Haddon, R. C. *Science* **1998**, *282*, 95.
(23) Kamaras, K.; Itkis, M. E.; Hu, H.; Zhao, B.; Haddon, R. C. *Science* **2003**, *301*, 1501.
(24) Hu, H.; Zhao, B.; Hamon, M. A.; Kamaras, K.; Itkis, M. E.; Haddon, R. C. *J. Am. Chem. Soc.* **2003**, *125*, 14893.
(25) Strano, M. S.; Dyke, C. A.; Usrey, M. L.; Barone, P. W.; Allen, M. J.; Shan, H.; Kittrell, C.; Hauge, R. H.; Tour, J. M.; Smalley, R. E. *Science* **2003**, *301*, 1519.
(26) Holzinger, M.; Vostrowsky, O.; Hirsch, A.; Hennrich, F.; Kappes, M.; Weiss, R.; Jellen, F. *Angew. Chem., Int. Ed.* **2001**, *40*, 4002.
(27) Holzinger, M.; Abraham, J.; Whelan, P.; Graupner, R.; Ley, L.; Hennrich, F.; Kappes, M.; Hirsch, A. *J. Am. Chem. Soc.* **2003**, *125*, 8566.
(28) Bettinger, H. F. *Org. Lett.* **2004**, *6*, 731.
(29) Chen, Z.; Nagase, S.; Hirsch, A.; Haddon, R. C.; Thiel, W.; Schleyer, P. v. R. *Angew. Chem., Int. Ed.* **2004**, *43*, 1552.
(30) Dag, S.; Gülseren, O.; Yildirim, T.; Ciraci, S. *Phys. Rev. B* **2003**, *67*, 165424.
(31) Frisch, M. J.; Trucks, G. W.; Schlegel, H. B.; Scuseria, G. E.; Robb, M. A.; Cheeseman, J. R.; Montgomery, J. A., Jr.; Vreven, T.; Kudin, K. N.; Burant, J. C.; Millam, J. M.; Iyengar, S. S.; Tomasi, J.; Barone, V.; Mennucci, B.; Cossi, M.; Scalmani, G.; Rega, N.; Petersson, G. A.; Nakatsuji, H.; Hada, M.; Ehara, M.; Toyota, K.; Fukuda, R.; Hasegawa, J.; Ishida, M.; Nakajima, T.; Honda, Y.; Kitao, O.; Nakai, H.; Klene, M.; Li, X.; Knox, J. E.; Hratchian, H. P.; Cross, J. B.; Adamo, C.; Jaramillo, J.; Gomperts, R.; Stratmann, R. E.; Yazyev, O.; Austin, A. J.; Cammi, R.; Pomelli, C.; Ochterski, J. W.; Ayala, P. Y.; Morokuma, K.; Voth, G. A.; Salvador, P.; Dannenberg, J. J.; Zakrzewski, V. G.; Dapprich, S.; Daniels, A. D.; Strain, M. C.; Farkas, O.; Malick, D. K.; Rabuck, A. D.; Raghavachari, K.; Foresman, J. B.; Ortiz, J. V.; Cui, Q.; Baboul, A. G.; Clifford, S.; Cioslowski, J.; Stefanov, B. B.; Liu, G.; Liashenko, A.; Piskorz, P.; Komaromi, I.; Martin, R. L.; Fox, D. J.; Keith, T.; Al-Laham, M. A.; Peng, C. Y.; Nanayakkara, A.; Challacombe, M.; Gill, P. M. W.; Johnson, B.; Chen, W.; Wong, M. W.; Gonzalez, C.; Pople, J. A. *Gaussian 03*, revision B.4; Gaussian, Inc.: Pittsburgh, PA, 2003.
(32) Perdew, J. P.; Burke, K.; Ernzerhof, M. *Phys. Rev. Lett.* **1996**, *77*, 3865.
(33) Perdew, J. P.; Burke, K.; Ernzerhof, M. *Phys. Rev. Lett.* **1997**, *78*, 1396(E).
(34) Haddon, R. C. *J. Phys. Chem. A* **2001**, *105*, 4164.